The geometric formulas of the Lewis's law and Aboav-Weaire's law in two dimensions based on ellipse packing

Kai Xu

Fisheries College, Jimei University, Xiamen, 361021, China

Email: kaixu@jmu.edu.cn

Abstract

The two-dimensional (2D) Lewis's law and Aboav-Weaire's law are two simple formulas derived from empirical observations. Numerous attempts have been made to improve the empirical formulas. In this study, we simulated a series of Voronoi diagrams by randomly disordered the seed locations of a regular hexagonal 2D Voronoi diagram, and analyzed the cell topology based on ellipse packing. Then, we derived and verified the improved formulas for Lewis's law and Aboav-Weaire's law. Specifically, we found that the upper limit of the second moment of edge number is 3. In addition, we derived the geometric formula of the von Neumann-Mullins's law based on the new formula of the Aboav-Weaire's law. Our results suggested that the cell area, local neighbor relationship, and cell growth rate are closely linked to each other, and mainly shaped by the effect of deformation from circle to ellipse and less influenced by the global edge distribution.

Introduction

From atomic to astronomic scales, the omnipresence of trivalent 2D structures have increasingly drawn broad and intense scientific interest (Weaire & Rivier 1984; Zsoldos et al. 2004). Understanding the cellular topology of these structures is fundamental for numerous scientific fields. Two empirical laws, the Lewis's law and the Aboav-Weaire's law, were used to describe the relationships between the edge number (n) and the cell area (A), and between n and the average edge number (m) of neighbor cells of the n-edged cell, respectively (Aboav 1970; Lewis 1926; Lewis 1928; Weaire 1974; Weaire & Rivier 1984). Recently, based on investigations on ten different kinds of natural and artificial 2D materials, Xu (2019) found that the cells can be classified as an ellipse's inscribed polygon (EIP) and tended to form the ellipse's maximal inscribed polygon (EMIP). This phenomena was named as ellipse packing, which is a short-range order shaped the 2D

PeerJ Preprints | https://doi.org/10.7287/peerj.preprints.27797v2 | CC BY 4.0 Open Access | rec: 18 Jun 2019, publ: 18 Jun 2019

topology by working together with the other short-range order, the trivalent vertices.

The Aboav-Weaire's law reads:

$$m = (6-\beta) + \frac{6\beta + \mu_2}{n}, \tag{1}$$

where six is the average edge number of polygonal cells, β is a constant, and μ_2 is a variance related to the edge distribution of cells (Weaire & Rivier 1984). Then, nm is the total edge number of neighbor cells of the n-edged cell. Besides, the Weaire's sum rule suggested $\mu_2 = \langle nm \rangle - 36 = \langle n^2 \rangle - 36$, which indicates that $\mu_2 \geq 0$ and μ_2 will increase with the edge range. Xu (2019) found that β is actually a variance and equals to the ratio of major axis to minor axis of the fitted ellipse. Besides, the β and μ_2 describe the deformation degrees from circle to ellipse, and from EMIP to EIP, respectively. Then, Eq. (1) can be rewritten as

$$nm = \left(6 - \frac{a}{b}\right) \times \mathrm{n} + \frac{6a}{b} + \mu_2, \tag{2}$$

where a and b are the semi-major axis and semi-minor axis of the fitted ellipse, respectively.

However, in the above study, the basic geometric data of ten kinds of 2D structures, such as coordinates of vertices, edge number, and cell area, were derived from the images (Xu 2019). This kind of data collection may affect the analysis, for example, it is very difficult to separate points and very short edges (Xu et al. 2017). To improve the analysis, we simulated a series of Voronoi diagrams by randomly disordering the seed locations of a regular hexagonal 2D structure following two previous studies (Zheng et al. 2005; Zhu et al. 2001).

Methods.

The coordinates of seed of the i-th Voronoi polygonal cell are

$$\begin{cases} X_i = X_{i0} + k \times d_0 \times \cos\theta_i \times \varphi_i \\ Y_i = Y_{i0} + k \times d_0 \times \sin\theta_i \times \varphi_i \end{cases}, \tag{3}$$

where $(X_{i0},\ Y_{i0})$ are the coordinates of the i-th seed of the regular hexagonal 2D structure, $(X_i,\ Y_i)$ are the corresponding coordinates after distortion, d_0 is the distance of two neighbor seeds of the regular hexagonal 2D structure, θ_i is a random angle $(0 \leq \theta_i \leq 2\pi)$, φ_i is a random number $(-1 \leq \varphi_i \leq 1)$, and k is the irregularity of the disordered Voronoi diagram (Zheng et al. 2005; Zhu et al. 2001). When $k = 0$, the Voronoi diagram was tiled by equal-size regular hexagons. The Voronoi diagrams were generated by R software (version 3.5.3) with deldir package (Lee & Schachter 1980). The coordinates of vertices, n, nm and real (measured) area (A_R) of each cell were extracted for the following analysis. For each polygonal cell, we used the R software (version 3.5.3) with the Conicfit package to fit an ellipse based on the coordinates of vertices (Chernov et al. 2014; Xu 2019). The area of the maximal inscribed polygon of the fitted ellipse (A_{MIP}) was calculated as $A_{MIP} = 0.5nabsin(2\pi/n)$ (Su 1987).

Results and discussion

Our data clearly showed that, regardless of increasing k, the average n and average A_R were very stable (Fig. 1A-B). The average nm, μ_2, and a/b increased with k (Fig. 1C-E), but the average A_R/A_{MIP} exhibited opposite trend (Fig. 1F). In this study, we confirmed that μ_2 could describe the deformation degree from EMIP to EIP which proposed by Xu (2019). Based on our data, we found the following equation

$$\mu_2 = \left(1 - \frac{A_R}{A_{MIP}} - \varepsilon\right) \times n, \tag{4}$$

where ε is a very small variance with unclear meaning. Then, the cell area can be calculated as

$$A_C = \left(1 - \frac{\mu_2}{n} - \varepsilon\right) \times A_{MIP}, \tag{5}$$

where A_C is the calculated cell area. Two previous studies which simulated Voronoi diagrams based on the same method as the present study also found that the μ_2 increased with k (Zheng et al. 2005; Zhu et al. 2001). Other studies suggested that the upper limit of μ_2 is infinite (Weaire & Rivier 1984; Zsoldos et al. 2004). When $k = 0.1$, all the cells became six-edged EIPs, then $\mu_2 = 0$ and A_C was very close to but still less than A_{MIP}. Thus, we proposed $\varepsilon > 0$. However, according to Eq. (4), the maximal value of μ_2 is the minimal value of n in a given Voronoi diagram. Therefore, $0 \leq \mu_2 < 3$. Because the ε is neglectable, Eq. (5) can be approximately expressed as following:

$$A_C \approx \left(1 - \frac{\mu_2}{n}\right) \times A_{MIP}. \tag{6}$$

Using Eq. (6), nm can be approximately calculated as

$$nm \approx \left(6 - \frac{a}{b}\right) \times n + \frac{6a}{b} + \left(1 - \frac{A_R}{A_{MIP}}\right) \times n, \tag{7}$$

The values of calculated nm (nm_C) using Eq. (2) and (7) were very close to each other and to the real (measured) nm (nm_R) (Fig. 1G). The average ratio of nm_C/nm_R calculated by Eq. (2) was 1.00±0.04 (2039 cells were analyzed), and 90% of the ratios were concentrated in range of 0.94 to 1.07 (Datasheet S1). The values of A_C calculated using Eq. (6) were also very close to that of A_R (Fig. 1H). The average ratio of A_C/A_R was 1.04±0.19 (2039 cells were analyzed), and 90% of the ratios were concentrated in range of 0.83 to 1.41.

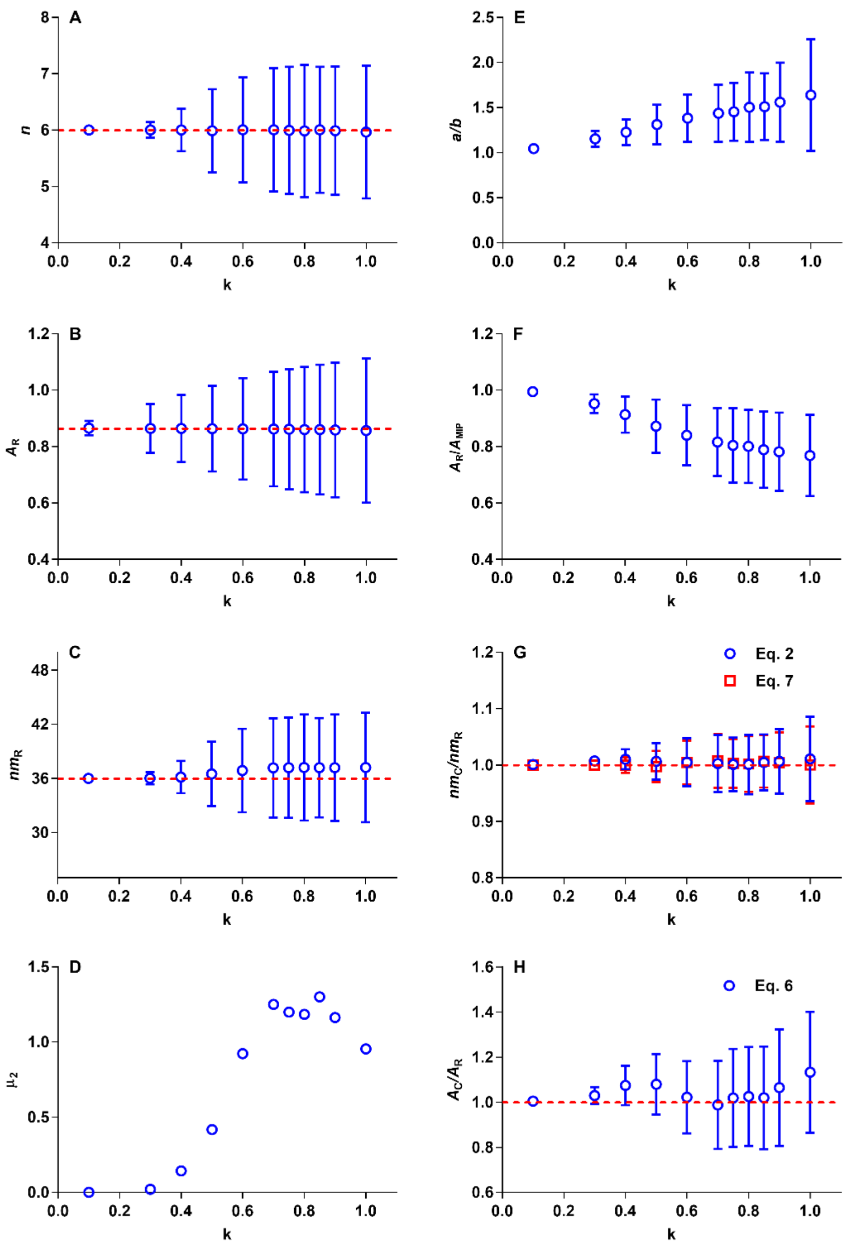

Figure 1 Relationships between k and geometric parameters of Voronoi diagrams. (A) Edge number n. (B) Real cell area A_R. (C) Real total edge number of neighbors nm_R. (D) The second moment of edge distribution of cells μ_2. (E) Ratio of semi-major axis and semi-minor axis a/b. (F) Ratio of A_R and A_{MIP} (The maximal area of inscribed polygon of fitted ellipse). (G) Ratio of nm_C (The calculated total edge number of neighbors) and nm_R. We used Eq. (2) and (7) to calculate nm_C. (H) Ratio of A_C (The calculated cell area) and A_R. We used Eq. (6) to calculate A_C.

Xu (2019) suggested that the regular hexagonal 2D structure is a specific case of 2D structure which is tiled by EMIPs. When k increased to 0.6, the a/b and A_R/A_{MIP} of the disordered Voronoi diagrams were very close to the random-seeded Voronoi diagrams (Xu 2019). Thus, the regular hexagonal 2D structure also can be considered as a specific case of Voronoi diagram. Combine the results of this study and the previous study by Xu (2019), we divided the 2D structures into two categories (Table 1):

Table 1 Summary of tile patterns and corresponding geometric formulas. a and b are the semi-major axis and semi-minor axis of fitted ellipse of an n-edged cell, respectively; and μ_2 is the second moment of the edges of the cells; ε is a very small variance.

Type	Tile pattern	A_C	nm
I	Tile with EMIPs	$0.5nabsin\left(\frac{2\pi}{n}\right)$	$nm = n\left(6-\frac{a}{b}\right)+\frac{6a}{b}+\mu_2$
II	Tile with EIPs	$0.5nabsin\left(\frac{2\pi}{n}\right)\left(1-\frac{\mu_2}{n}-\varepsilon\right)$	

Based on the above theoretical frame, we improved the summary on the variations of 2D topology which proposed by Xu (2019). Assuming a trivalent 2D structure contains constant number of vertices, and each time change only one global parameter, then there are two kinds of basic topological variations (Table 2): V1. μ_2-variation, which will not change the type and the area of 2D structure, all the other parameters will be changed. For instance, the transition between crystalline and amorphous SiO_2 film (Büchner & Heyde 2017; Büchner et al. 2016; Xu 2019), and between the regular hexagonal and disordered Voronoi diagrams which reported by the present study and the previous studies (Zheng et al. 2005; Zhu et al. 2001). V2. Scaling, which will change the ab, area of 2D structure and cells, but μ_2, n, and nm will not be changed. Besides, the non-uniform scaling will change the a/b.

Table 2 Two kinds of basic topology variations of 2D structures. Symbol × represents the parameter will not be changed, and √ represents the parameter will be changed.

	Global parameters		Local parameters				
	Area of 2D structure	μ_2	n	Cell area	ab	a/b	nm
V1	×	√	√	√	√	√	√
V2	√	×	×	√	√	× or √	×

The non-living and living 2D materials are generally belong to the Type I and II 2D structures, respectively (Xu 2019). To obey ellipse packing, the topological variations of Type I 2D structure need to be achieved by global adjustment (Büchner & Heyde 2017; Xu 2019); and that for Type II 2D structure can be achieved by local fine-turning, e.g. the division related allometric growth of cell edges of biological 2D structure (Xu 2019; Xu et al. 2017). The cell growth kinetics of 2D structure also gained numerous scientific attentions. The rate of area change of an n-edged cell is given by the well-known physical formula of the von Neumann-Mullins's law (Mullins 1956):

$$\frac{\mathrm{d}A}{\mathrm{d}t} = \frac{\pi k}{3}(n-6), \tag{8}$$

where A is the cell area, k is the reduced cell boundary mobility. The Eq. (8) is generally used to describe the cell growth kinetics of Type II 2D structures, such as, soap, mollusc shells (Zöllner & Zlotnikov 2018). This equation suggests that the area of cells with more than six edges increase, while cells with fewer than six edges shrink and cells with six edges are stable. The geometric formula of the von Neumann-Mullins's law could be derived from the Aboav-Weaire's law:

$$\frac{\mathrm{d}A}{\mathrm{d}t} = n - m = (n-6)\left(1+\frac{a}{nb}\right) - \frac{\mu_2}{n}. \tag{9}$$

Briefly, the Eq. (8) and (9) are the same when come to predict the relationship between cell growth rate and edge number. A recent study suggested that the simulated values of $\pi k/3$ were ranged from 1.0036 to 1.0290, which matched very well with the theoretical value of $\pi/3$ (Zöllner & Zlotnikov 2018). The average a/b of shells and soap was about 1.1 (Xu 2019), then the average value of $1 + a/(nb)$ agreed well with the $\pi k/3$. Based on Eq. (9), for six-edged cells, the cell growth rate equals to 0 when $\mu_2 = 0$; while cell area will slowly decrease when $\mu_2 > 0$. That is because the m of six-edged cells is just slightly higher than six, according to the improved formula (Eq. (2)) of Aboav-Weaire's law. The Eq. (9) describes the effects of local neighbor relationship and global edge distribution on cell growth rate. Further study is needed to test the Eq. (9). Besides, to date, no such kind of equation is established for Type II 2D material, especially for the biological 2D structures.

Conclusion

This study generated a series of Voronoi diagrams by randomly disordered a regular hexagonal Voronoi diagram and derived new geometric formulas for Lewis's law and Aboav-Weaire's law based on the cell topological parameters. This study also derived a geometric formula for the von Neumann-Mullins's law on the basis of the new formula of the Aboav-Weaire's law. The present study suggested that the cell area, local neighbor relationship, and cell growth rate could be calculated using the edge number, semi-axes of fitted ellipse, and the second moment of edge distribution. Furthermore, the cell area, local neighbor relationship, and cell growth rate are mainly determined by the deformation effects of circle and less influenced by the global edge distribution. Based on Lewis's law, this study found that the upper limit of the second moment of edge distribution is 3.

Acknowledgments

The author thanks Prof. Rolf Turner for the development of R package deldir and his technical support. The author also thanks Miss Fangyu Guo and Ping Zhang for their assistance collecting the geometric data of the cells. Thanks my beloved wife Huimin Cheng for her support. This work was supported by the National Key Research and Development Program of China (2018YFD0900702).

References

Aboav DA. 1970. The arrangement of grains in a polycrystal. *Metallography* 3:383-390.
Büchner C, and Heyde M. 2017. Two-dimensional silica opens new perspectives. *Progress in Surface*

Science 92:341-374. 10.1016/j.progsurf.2017.09.001

Büchner C, Liu L, Stuckenholz S, Burson KM, Lichtenstein L, Heyde M, Gao H-J, and Freund H-J. 2016. Building block analysis of 2D amorphous networks reveals medium range correlation. *Journal of Non-Crystalline Solids* 435:40-47. 10.1016/j.jnoncrysol.2015.12.020

Chernov N, Huang Q, and Ma H. 2014. Fitting quadratic curves to data points. *British Journal of Mathematics & Computer Science* 4:33-60.

Lee D-T, and Schachter BJ. 1980. Two algorithms for constructing a Delaunay triangulation. *International Journal of Computer & Information Sciences* 9:219-242.

Lewis FT. 1926. The effect of cell division on the shape and size of hexagonal cells. *The Anatomical Record* 33:331-355.

Lewis FT. 1928. The correlation between cell division and the shapes and sizes of prismatic cells in the epidermis of cucumis. *The anatomical record* 38:341-376.

Mullins WW. 1956. Two-dimensional motion of idealized grain boundaries. *Journal of Applied Physics* 27:900-904. 10.1063/1.1722511

Su H. 1987. The characteristics of maximum inscribed and minimum circumscribed polygons of ellipse. *Teaching Mathematics* 6:22-26.

Weaire D. 1974. Some remarks on the arrangement of grains in a polycrystal. *Metallography* 7:157-160.

Weaire D, and Rivier N. 1984. Soap, cells and statistics—random patterns in two dimensions. *Contemporary Physics* 25:59-99. 10.1080/00107518408210979

Xu K. 2019. Ellipse packing in two-dimensional cell tessellation: a theoretical explanation for Lewis's law and Aboav-Weaire's law. *PeerJ* 7:e6933. 10.7717/peerj.6933

Xu K, Xu Y, Ji D, Chen T, Chen C, and Xie C. 2017. Cells tile a flat plane by controlling geometries during morphogenesis of *Pyropia* thalli. *PeerJ* 5:e3314. 10.7717/peerj.3314

Zheng Z, Yu J, and Li J. 2005. Dynamic crushing of 2D cellular structures: A finite element study. *International Journal of Impact Engineering* 32:650-664. 10.1016/j.ijimpeng.2005.05.007

Zhu HX, Thorpe SM, and Windle AH. 2001. The geometrical properties of irregular two-dimensional Voronoi tessellations. *Philosophical Magazine A* 81:2765-2783. 10.1080/01418610010032364

Zöllner D, and Zlotnikov I. 2018. Modelling texture dependent grain growth by 2D Potts model simulations: A detailed analysis. *Computational Materials Science* 155:180-196. 10.1016/j.commatsci.2018.08.044

Zsoldos I, Réti T, and Szasz A. 2004. On the topology of 2D polygonal and generalized cell systems. *Computational Materials Science* 29:119-130. 10.1016/j.commatsci.2003.08.035